

Studying Spin-Orbit Dynamics using Measurements of the Proton's Polarized Gluon Asymmetry

Yevgeny Binder¹

Quantum Code, Buffalo Grove, IL 60089

and Physics Department, Loyola University, Chicago, IL 60626

Gordon P. Ramsey²

Physics Department, Loyola University, Chicago, IL 60626

and High Energy Physics Division, Argonne National Lab, Argonne, IL 60439

Dennis Sivers

Portland Physics Institute, Portland, OR 97239

and Spin Physics Center, University of Michigan, Ann Arbor, MI 48103

Abstract

Measurements involving the gluon spin density, $\Delta G(x, t) \equiv G_{++}(x, t) - G_{+-}(x, t)$, can play an important role in the quantitative understanding of proton structure. To demonstrate this, we show that the shape of the gluon asymmetry, $A(x, t) \equiv \Delta G(x, t)/G(x, t)$, contains significant dynamical information about non-perturbative spin-orbit effects. It is instructive to use a separation $A(x, t) = A_0^\epsilon(x) + \epsilon(x, t)$, where $A_0^\epsilon(x)$ is an approximately scale invariant form that can be calculated within a given factorization prescription from the measured distributions, $\Delta q(x, t)$, $q(x, t)$ and $G(x, t)$. Applying this separation with the $J_z = \frac{1}{2}$ sum rule provides a convenient way to determine the amount of orbital angular momentum generated by mechanisms associated with confinement and chiral dynamics. The results are consistent with alternate non-perturbative approaches to the determination of orbital angular momentum in the proton. Our studies help to specify the accuracy that future measurements should achieve to constrain theoretical models for nucleon structure.

¹Work supported in part by a Mulcahy Undergraduate Research Scholarship, Loyola University Chicago

²Work supported by the U.S. Department of Energy, Division of High Energy Physics, Contract DE-AC02-06CH11357. E-mail: gpr@hep.anl.gov

1 Introduction

Several experimental programs [1, 2, 3, 4, 5] have devised strategies aimed at providing a significant measure of the proton's spin weighted gluon density,

$$\Delta G(x, t) \equiv G_{++}(x, t) - G_{+-}(x, t), \quad (1)$$

where x is the Bjorken scaling variable and $t \equiv \log[\alpha_s(Q_0^2)]/\log[\alpha_s(Q^2)]$ is the Q^2 evolution variable. The interest in these measurements is often framed in terms of arguments using the $J_z = \frac{1}{2}$ sum rule, [6]

$$J_z = \frac{1}{2} \equiv \frac{1}{2} \langle \Delta \Sigma(t) \rangle + \langle \Delta G(t) \rangle + L_z(t), \quad (2)$$

where

$$\begin{aligned} \langle \Delta \Sigma(t) \rangle &\equiv \int_0^1 dx \Delta q(x, t) \quad \text{and} \\ \langle \Delta G(t) \rangle &\equiv \int_0^1 dx \Delta G(x, t) \end{aligned} \quad (3)$$

are the projections of the spin carried by all quarks and the gluons on the helicity (or z)-axis, respectively. Also $L_z(t)$ is the net z -component of the orbital angular momentum of the constituents. In this analysis, we will not attempt to identify independent flavor components of $L_z(t)$ within the sum rule. Arguments concerning the content and assumptions involved in such separations have been presented by Jaffe and Manohar [7] and by Ji. [8] Since these theoretical considerations do not impact the content of the analysis in sections 1 and 2, we will defer to the subject of separating quark and gluon orbital angular momenta until section 3, where we discuss specific models for proton structure.

The t -evolution of the terms on the RHS of equation (2) adds some content to this discussion. It was shown in [6] that the lowest order QCD evolution equation leads to $\partial \Sigma / \partial t = 0$ in the chiral factorization prescription, reflecting the underlying helicity conservation of QCD perturbation theory. It was also shown that for a large range of boundary conditions, $\partial \Delta G / \partial t > 0$, so that the sum rule (2) would seem to lead to the conclusion that

$$\lim_{t \rightarrow \infty} \langle \Delta G(t) \rangle \rightarrow +\infty \quad (4)$$

$$\lim_{t \rightarrow \infty} L_z(t) \rightarrow -\infty. \quad (5)$$

The reconciliation of this result within the framework of perturbative QCD was achieved by Ratcliffe [9], who showed that the structure of the DGLAP evolution equations [10] is based upon an iteration of perturbative processes in which a change of $\Delta G = \pm 1$ is balanced by a corresponding change of $L_z = \mp 1$. The chiral structure of QCD therefore implies that a helicity-sensitive probe of the proton's gluon density uncovers Q^2 dependence from Ratcliffe resolution structures that can be considered perturbatively generated P-wave color correlations of the composite system. Higher order evolution [10] makes small modifications to Ratcliffe's result without diminishing its basic content. Recent papers by Bakker, Leader and Trueman [11] and by Chen and Ji, [12] have clarified the understanding of angular momentum sum rules by dealing with some of the complications associated with the non-local properties of orbital angular momentum.

Recent DIS experiments [13, 14] have significantly lowered the measurement errors of the quark spin contribution ($\Delta\Sigma$) to equation (2). The COMPASS collaboration analysis quotes a result

$$\langle \Delta\Sigma \rangle = 0.30 \pm 0.01(\text{stat}) \pm 0.02(\text{evol}), \quad \text{all data} \quad (6)$$

while the HERMES collaboration analysis quotes a result

$$\langle \Delta\Sigma \rangle = 0.330 \pm 0.025(\text{exp}) \pm 0.011(\text{th}) \pm 0.028(\text{evol}), \quad \text{all data.} \quad (7)$$

These values can be used with the $J_z = \frac{1}{2}$ sum rule to evaluate the impact of existing and potential gluon asymmetry measurements.

Recent experimental results sensitive to $\Delta G(x, t)$ and the gluon asymmetry, $A(x, t) \equiv \Delta G(x, t)/G(x, t)$ have provided important new information. Although the analysis of these experiments is limited in sensitivity and range of $\langle x \rangle$, the results suggest the possibility that at some small x and Q_0^2 , $\Delta G(x, t_0) \leq 0$. Understanding the shape of $\Delta G(x, t)$ for the whole range $x \in (0, 1)$ is important, since the asymptotic result

$$\lim_{t \rightarrow \infty} \alpha_s(t) \langle \Delta G(t) \rangle = \text{constant} \quad (8)$$

follows from the full QCD evolution equations, where the constant could be positive, negative or zero as $t \rightarrow \infty$. These measurements suggest that phenomenological conclusions described in equations (5) may be in error and the asymptotic color structure of the proton is quite different from what has been previously supposed. If the constant in equation (8) is zero,

then $\langle \Delta G(t) \rangle$ and $L_z(t)$ should asymptotically approach constants, while if it is negative, then the signs of equations (5) should be switched. Thus, experimental evidence on $\Delta G(x, t_0)$ for a limited range of x and t_0 must be combined with an extrapolation in order to specify the nature of $\langle \Delta G(t) \rangle$ and $L_z(t)$ at large t . The experimental results alone are not conclusive. The specific approach in this paper helps to illuminate these possibilities and to fix onto crucial experimental results.

From the discussion above, it is instructive to write the polarized gluon asymmetry using the decomposition

$$A(x, t) \equiv \Delta G(x, t)/G(x, t) = A_0^\epsilon(x) + \epsilon(x, t), \quad (9)$$

where $A_0^\epsilon(x)$ is dependent only upon x , calculable in PQCD by the using definition

$$A_0^\epsilon(x) \equiv \left[\left(\frac{\partial \Delta G(x, t)}{\partial t} \right) / \left(\frac{\partial G(x, t)}{\partial t} \right) \right]. \quad (10)$$

The numerator and denominator on the right side of equation (10) are calculable from the DGLAP equations and each depends strictly upon x via the respective convolutions. [10] The small correction, $\epsilon(x, t)$ describes shape-dependent differences in the evolutions of $G(x, t)$ and $\Delta G(x, t)$ at leading order (LO) in QCD perturbation theory. Differentiating $A(x, t)$ with respect to t in equation (9) and using the scale-invariance of $A_0^\epsilon(x)$, it follows that

$$\frac{\partial}{\partial t} [\epsilon(x, t) G(x, t)] = 0.$$

The expression (9) for $A(x, t)$ at some initial $t = t_0$ leads to an equivalent decomposition for $\Delta G(x, t)$ in the form

$$\Delta G(x, t_0) = A_0^\epsilon(x) \cdot G(x, t_0) + \Delta g_\epsilon(x) \quad (11)$$

where the “polarized gluon excess”, $\Delta g_\epsilon(x)$, is given by

$$\Delta g_\epsilon(x) = \epsilon(x, t) \cdot G(x, t) \quad (12)$$

and is t -independent. This provides a boundary condition for the partial differential equation (10) that defines $A_0^\epsilon(x)$ and can be used to characterize possible different shapes for $A(x, t)$ in equation (9). This boundary condition for the partial differential equation (10) occurs at an unphysical region in that the decomposition in (11) cannot be valid when

$G(x, t_0) = 0$. In practice, this means that there are nontrivial constraints on the magnitude of $\Delta g_\epsilon(x)$. We will discuss these constraints when we consider explicit solutions to equation (10).

In this paper, we will neglect the t -dependence of $\Delta\Sigma(x, t)$ at LO and concentrate on an alternate approach to characterizing the consequences of the t -dependence of $\Delta G(x, t)$. Using the current data for $\Delta\Sigma$ as input, we combine equations (2), (6) and (7) to write

$$L_z(t) + \langle \Delta G(t) \rangle \approx \frac{1}{2}(1 - \langle \Delta\Sigma \rangle) \approx 0.34 \pm 0.02 \quad (13)$$

in a chiral factorization prescription. The quoted error is entirely due to the data uncertainties in equations (6) and (7). The asymmetry $A(x, t)$ is parameterized as outlined in Section 2 and the corresponding polarized gluon obtained from equation (9) is substituted into equation (13) to determine a value for the orbital angular momentum, $L_z(t)$. Our approach to the study of $\Delta G(x, t)$ is largely complementary to the usual global analysis determination discussed, for example, by Hirai and Kumano [15] and others [16, 17] where the main input for $\Delta G(x, t)$ involves measurement of the scaling violations for $\Delta q(x, t)$. Since it is highly unlikely that future experiments sensitive to $\Delta G(x, t)$ will determine this distribution with an accuracy similar to that found in the determination of Δq or to that of $G(x, t)$ and $q(x, t)$, our method takes into account the similarities between the evolution of $\Delta G(x, t)$ and $G(x, t)$ to provide the necessary extrapolations to all x . Using knowledge of $\Delta q(x, t)$ along with $q(x, t)$ and $G(x, t)$ data sensitive to values of $\Delta G(x, t)$ in limited regions of x and t can then be used efficiently to obtain valid estimates for $L_z(t)$. In particular, as long as $G(x, t_0)$ is large enough at small scales, t_0 , associated with confinement and chiral dynamics, $L_z(t)$ can also be extrapolated to provide a measure of spin-orbit dynamics at such scales.

The possibility that there could exist a scale-invariant form for the gluon polarization asymmetry, $A(x, t)$, was first considered by Einhorn [18] on the basis of numerical studies of the LO DGLAP equations. [10] The work of reference [19] explores Einhorn's suggestion by showing that a scale-invariant form for $A_0^\epsilon(x)$ is a feature of the Close-Sivers Bremsstrahlung model. Scale-invariance occurs in that approach because the perturbative diagrams which determine the t -evolution of the gluon distributions are the same as those that distribute the spin information to the gluons at LO. The papers of references [20]-[23] have significantly expanded the phenomenological study of the information contained in the shape of $A(x, t)$

by introducing the connection to the $J_z = 1/2$ sum rule and by considering the possibility of small fluctuations around the scale-invariant form described in equations (9), (11) and (12).

The remainder of this paper is organized as follows. In Section 2 we discuss how equation (10) leads to a non-linear equation for $A_0^\epsilon(x)$ based on the DGLAP equations. We then generate parameterizations of $A_0^\epsilon(x)$ in leading-order (LO) and outline the next-to-leading order (NLO) calculation. These parameterizations can give a meaningful description of $A(x, t)$ or $\Delta G(x, t)$ with suitable constraints on $\epsilon(x, t)$ or $\Delta g_\epsilon(x)$ respectively. When the constraints are satisfied, a complete description of $A_0^\epsilon(x)$ is obtained from boundary conditions combined with existing measurements of the singlet quark and unpolarized gluon densities, $q(x, t)$, $\Delta q(x, t)$ and $G(x, t)$. Section 3 presents numerical determination of $A_0^\epsilon(x)$ within these constraints and the observation that preliminary data on $\Delta G(x, t)$ from several measurements are within these bounds. This suggests that future measurements of $\Delta G(x, t)$ or $A(x, t)$ with improved accuracy can be used in conjunction with our analysis to determine a low energy non-perturbative component of orbital angular momentum. Section IV includes a brief discussion of the importance of understanding the constituent orbital angular momentum in a composite system and how the $J_z = \frac{1}{2}$ sum rule and measurements sensitive to $A(x, t)$ can provide important constraints on dynamical models for proton structure.

2 The Scale-Invariant Gluon Asymmetry $A_0^\epsilon(x)$

2.1 Numerical approach to the gluon asymmetry

The solution of equations based on equations (9) and (10) was proposed by Ramsey and Sivers [21-23]. The calculation of the asymmetry provided a method to determine ΔG without theoretical biases on its shape. This was followed by analysis of the relation between the Δg_ϵ parameterizations and the corresponding range of possible L_z [21]. Since new data for the asymmetry have been made available, this method has allowed us to refine the range of possible $\langle \Delta G \rangle$ and L_z consistent with this data [22, 23]. The culmination of this work is presented in this paper.

In this section, we create a numerical mechanism which allows phenomenological determination of the non-perturbative quantity L_z from the experimental measurements of

ΔG and $\frac{\Delta G}{G}$. This is done without an a priori assumption for the polarized glue. We will outline a numerical approach to calculate the asymmetry- L_z connection in order to provide a self-consistency check to this approach and provide a range of possible values for the orbital angular momentum.

The perturbative component of the polarized gluon asymmetry $A_0^\epsilon(x)$ can be calculated from a parameterization of the correction $\Delta g_\epsilon(x)$ by inserting equation (11) into the expression (10) for $A_0^\epsilon(x)$. Then equation (10) can then be solved using $\partial\Delta G/\partial t$ and $\partial G/\partial t$ given by DGLAP evolution. In kinematic regions where the DGLAP evolution equations are valid, equation (10) allows one to generate $A_0^\epsilon(x)$ by

$$A_0^\epsilon(x) = \left[\frac{\Delta P_{gq} \otimes \Delta q + \Delta P_{gg} \otimes (\Delta G)}{P_{gq} \otimes q + P_{gg} \otimes G} \right], \quad (14)$$

where the convolution is defined as $P(x) \otimes Q(x) \equiv \int_0^1 \frac{dy}{y} P(y) Q(x/y)$. Then equations (10) and (11) can be used to generate the corresponding asymmetry using the DGLAP equations via the iterative equation

$$A_0^\epsilon(x) = \left[\frac{\Delta P_{Gq} \otimes \Delta q + \Delta P_{GG} \otimes [A_0^\epsilon \cdot G + \Delta g_\epsilon]}{P_{Gq} \otimes q + P_{GG} \otimes G} \right]. \quad (15)$$

Since the $A_0^\epsilon(x)$ term occurs on both sides of the equation, we parametrize $A_0^\epsilon(x)$ and $\Delta g_\epsilon(x)$ subject to theoretical constraints and determine the coefficients of the parameterizations that satisfy equation (15). For each fixed parameterization of $\Delta g_\epsilon(x)$, the resulting asymmetry $A(x, t)$ and corresponding ΔG from equation (11) can then be checked for positivity with the corresponding unpolarized gluon at LO. The various parametrizations of $\Delta g_\epsilon(x)$ were chosen to have integrals over all x between -0.5 and 0.5 . The particular parametrization in the second line of Table 1 was selected to change sign, consistent with instanton models. This possibility was discussed by the HERMES collaboration and has not been ruled out by data. [1, 13, 15, 29] The process to determine the NLO corrections to the asymmetry is similar to that of LO with the appropriate corrections to the splitting functions and evolution parameters. This will be addressed shortly.

The calculation of $A_0^\epsilon(x)$ in equation (15) has been done using the CTEQ5 [24] and MRST [25] unpolarized parton distributions for comparison and the polarized quark distributions from reference [26]. All are evaluated at $Q_0^2 = 1 \text{ GeV}^2$ for the LO distributions. The

CTEQ5 unpolarized distributions are given by

$$\begin{aligned}
xu_v(x) &= 0.9783x^{0.4942}(1-x)^{3.3705}(1+10.0012x^{0.8571}) \\
xd_v(x) &= 0.5959x^{0.4942}(1-x)^{4.2785}(1+8.4187x^{0.7867}) \\
xS_{total}(x) &= 1.2214x^{0.0877}(1-x)^{7.7482}(1+3.389x) \\
xG(x) &= 3.3862x^{0.261}(1-x)^{3.4795}(1-0.9653x).
\end{aligned} \tag{16}$$

For this set, $\int_0^1 xG(x) dx = 0.28$, representing the momentum carried by the gluons. The MRST LO unpolarized distributions are

$$\begin{aligned}
xu_v(x) &= 0.6051x^{0.4089}(1-x)^{3.395}(1+2.078\sqrt{x}+14.56x) \\
xd_v(x) &= 0.05811x^{0.2882}(1-x)^{3.874}(1+34.69\sqrt{x}+28.96x) \\
xS_{total}(x) &= 0.2004x^{-0.2712}(1-x)^{3.808}(1+2.283\sqrt{x}+20.69x) \\
xG(x) &= 64.57x^{0.9171}(1-x)^{6.587}(1-3.168\sqrt{x}+3.251x).
\end{aligned} \tag{17}$$

For the MRST set, $\int_0^1 xG(x) dx = 0.35$, for comparison to the CTEQ5 set. In each case the total quark contribution is then given by:

$$xq_{total}(x) = xu_v(x) + xd_v(x) + xS_{total}(x). \tag{18}$$

The polarized distributions given by GGR [26] in terms of the unpolarized ones are

$$\begin{aligned}
x\Delta u_v(x) &= [1 + 0.25(1-x)^2/\sqrt{x}]^{-1}(xu_v(x) - 2xd_v(x)/3) \\
x\Delta d_v(x) &= [1 + 0.25(1-x)^2/\sqrt{x}]^{-1}(-xd_v(x)/3) \\
\Delta S_{total}(x) &= (-2.36 + 2.66\sqrt{x}) xS_{total}(x),
\end{aligned} \tag{19}$$

where

$$x\Delta\Sigma(x) = x\Delta u_v(x) + x\Delta d_v(x) + x\Delta S_{total}(x). \tag{20}$$

Although, in principle, we are sensitive to the shape of the unpolarized gluon distribution at Q_0^2 , the CTEQ and MRST only differ at small $x < 0.1$ and the effect on our results is minimal. For both unpolarized CTEQ and MRST distributions used in equation (15), the term in the denominator vanishes at a critical Bjorken- x value of approximately

$x_c \approx 0.20 \rightarrow 0.30$ at LO. To avoid this numerical problem, we take the denominator and terms with the asymmetry to one side, giving

$$A_0^\epsilon [P_{gq}^{LO} \otimes q + P_{gg}^{LO} \otimes G] - \Delta P_{gg}^{LO} \otimes (A_0^\epsilon \cdot G) = [\Delta P_{gq}^{LO} \otimes \Delta q + \Delta P_{gg}^{LO} \otimes (\Delta g_\epsilon)]. \quad (21)$$

This mitigates the problem of the point discontinuity in equation (15) and makes the determination of $A_0^\epsilon(x)$ straightforward. Since the asymmetry appears in both terms on the left hand side of the equation, a numerical trial-and-error technique must be used.

To establish an initial reference point for the solution of equation (21), practical constraints for the asymmetry at LO should include:

- strong positivity: $|A(x, t_0)| \leq 1$ for all $0 \leq x \leq 1$, and
- endpoint values: $A(0, t_0) = 0$ and $A(1, t_0) = 1$.

Simple positivity for the gluon asymmetry at LO requires $|A(x, t)| \leq 1$. Since the individual terms on the right side of equation (11) do not represent separate observables, the calculated $A_0^\epsilon(x)$ need not satisfy these criteria, but the full calculated asymmetry, $A(x, t)$ must. As a practical matter, the strong positivity constraint enforces the restriction that $\Delta g_\epsilon(x)$ is small and provides a tight restraint on the range of $\Delta g_\epsilon(x)$ for which stable solutions can be found. The constraint on endpoint values enforces the Brodsky-Farrar constituent counting rules as $x \rightarrow 1$ and the requirement that $\Delta G(x = 0, t)$ vanishes. In all solutions, the convolutions in (21) are dominated in the proton by the valence up quark as $x \rightarrow 1$.

To investigate possible asymmetry solutions, we start with an $A_0^\epsilon(x)$ parameterization in the form

$$A_0^\epsilon(x) \equiv Ax^\alpha - (B - 1)x^\beta + (B - A)x^{\beta+1}, \quad (22)$$

which automatically satisfies the endpoint constraints provided the exponents α and β are positive. This parameterization includes substantial flexibility in adjusting shapes while keeping the number of free parameters to a minimum. Using the CTEQ and MRST unpolarized distributions and the GGR polarized distributions given in equations (16) through (20) for the calculation, we find that only parameterizations of Δg_ϵ that conform to the condition

$$|< \Delta g_\epsilon >| \leq 0.25. \quad (23)$$

lead to solutions of equations (15) and (21) that satisfy the positivity constraint. A representative sample of the parameterizations whose asymmetries and corresponding polarized gluon distribution satisfy all the constraints are summarized in Table 1. These solutions give integrals $\langle \Delta G \rangle$ ranging from about -0.09 to 0.59 at these small $Q_0^2 = 1 \text{ GeV}^2$ values. Line two of the table contains the only non-monotonic parameterizations of Δg_ϵ that has been included in this sample. It should be noted that although some of the magnitudes of the integrated gluon distributions, $\langle \Delta G \rangle$, are less than those of $\langle \Delta g_\epsilon \rangle$, they occur for the parameterizations of Δg_ϵ whose integrals are negative or zero. Since this term is added to the overall polarized gluon distribution, the results are consistent with the model.

Table 1: Gluon Asymmetry Parameters at $Q_0^2 = 1 \text{ GeV}^2$

Δg_ϵ	$\langle \Delta g_\epsilon \rangle$	A_0^ϵ	$\langle \Delta G \rangle$
0	0	$3x^{1.5} - 3x^{2.2} + x^{3.2}$	0.28
$x(x - 0.25)(1 - x)^5$	0	$1.75x^{1.9} - 5x^{2.4} + 4.25x^{3.4}$	-0.01
$2(1 - x)^7$	0.25	$4x^{1.6} - 4x^{2.1} + x^{3.1}$	0.51
$-2(1 - x)^7$	-0.25	$1.75x^{1.1} - 1.5x^{2.1} + 0.75x^{3.1}$	0.18
$18x(1 - x)^7$	0.25	$2x^{1.8} - x^{2.5}$	0.39
$-18x(1 - x)^7$	-0.25	$2.25x^{1.7} - x^2 - 0.25x^3$	-0.09
$-90x^2(1 - x)^7$	-0.25	$3.5x^{1.3} - 4.5x^{2.2} + 2x^{3.2}$	0.25
$9x(1 - x)^7$	0.125	$3.75x^{1.4} - 3x^{1.6} + 0.25x^{2.6}$	0.40
$-9x(1 - x)^7$	-0.125	$3.25x^{1.4} - 3.75x^{2.2} + 1.5x^{3.2}$	0.25
$4.5x(1 - x)^7$	0.0625	$2x^{0.9} - 1.5x^{1.2} + 0.5x^{2.2}$	0.59
$-4.5x(1 - x)^7$	-0.0625	$2.25x^{1.1} - 2.25x^{1.9} + x^{2.9}$	0.43

The solutions for A_0^ϵ listed in Table 1 represent the best fit coefficients of equation (22) subject to roundoff error in solving equation (21). These parametrizations of A_0^ϵ are used to determine forms for $\Delta G(x, t)$ in equation (11) that can be tested experimentally in processes at large t for various ranges of x . The scale invariant nature of $\Delta g_\epsilon(x)$ implies that $\partial \Delta g_\epsilon / \partial t = 0$, so that the accuracy by which we can extract information on L_z can be

estimated. Expanding $\Delta g_\epsilon = \epsilon(x, t) \cdot G(x, t)$ in t :

$$\epsilon(x, t) \cdot G(x, t) = \epsilon(x, t_0) \cdot G(x, t_0) + \frac{\partial(\epsilon(x, t) \cdot G(x, t))}{\partial t} (t - t_0) + \frac{\partial^2(\epsilon(x, t) \cdot G(x, t))}{\partial t^2} (t - t_0)^2 + \dots \quad (24)$$

The second term on the right side vanishes identically and at LO and the second order term in equation (24) can be neglected, since second order terms in t may arise only at NLO and higher. Thus, at LO we can write

$$\Delta G(x, t) - \Delta G(x, t_0) \approx A_0^\epsilon(x) \cdot [G(x, t) - G(x, t_0)] + \mathcal{O}(\sqcup - \sqcup_\epsilon). \quad (25)$$

Thus, the polarized gluon distribution can be parametrized accurately at LO. All of the perturbatively generated orbital angular momentum can be extracted from the $J_z = 1/2$ sum rule within parton distribution uncertainties to this order. At LO, $\Delta \Sigma(x)$ is independent of t , so the amount of orbital angular momentum generated by Ratcliffe resolution structures in the range of scales (t, t_0) can be given by:

$$L_z(t) - L_z(t_0) = - \int_0^1 dx A_0^\epsilon \cdot [G(x, t) - G(x, t_0)] + \mathcal{O}(\sqcup - \sqcup_\epsilon). \quad (26)$$

Solving the nonlinear equation for $A_0^\epsilon(x)$ then leads to what we call the Ratcliffe – subtracted version of the $J_z = \frac{1}{2}$ sum rule, where the perturbatively generated orbital angular momentum and the perturbative evolution of $\Delta G(x, t)$ are subtracted. The separation allows for the measurement of $\Delta G(t)$ to be associated with a non-perturbative component of orbital angular momentum generated by the effects of chiral symmetry and confinement on proton structure. Using equations (13) and (26) we can write

$$L_z(t_0) = 0.34 \pm 0.02 - \langle \Delta G(t) \rangle + \langle A_0^\epsilon \cdot [G(x, t) - G(x, t_0)] \rangle + \mathcal{O}(\sqcup - \sqcup_\epsilon). \quad (27)$$

so that measurements sensitive to $\Delta G(x, t)$ at some large value of t can be used to estimate the amount of constituent orbital angular momentum present at smaller values of t in the perturbative region. For this study, we will choose $t_0 \equiv (t = 0)$ to correspond to $Q^2 = 1 \text{ GeV}^2$. This is a region where the DGLAP evolution is valid and processes evolved by BFKL evolution are not crucial to this study. It is also the kinematic region where chiral symmetry is broken. All parton distributions are evolved to this value.

Our preliminary studies into the numerical solutions to equation (21), as indicated in Table 1, demonstrate that such solutions are sensitive to both the shape of $\Delta g_\epsilon(x)$ and its

normalization, $|\langle \Delta g_\epsilon \rangle|$. This dual sensitivity arises because the region in x where the denominator of equation (15) is small, $x \in (0.24, 0.30)$, contributes significantly to $A_0^\epsilon(x)$ for all $x \leq 0.30$. The nonlinear nature of this equation makes the solution sensitive to the convolution term, $\Delta P_{gg}^{LO} \otimes \Delta g_\epsilon$ on the right side of (21). As indicated in the discussion above, the requirement in (23) limits the impact of the normalization. To further study the numerical shape of $\Delta g_\epsilon(x)$, we have separately examined solutions to (21) where the support of $\Delta g_\epsilon(x)$ was restricted to the large- x region, $x \geq 0.30$, or to the small- x region, $x \leq 0.20$.

These studies indicated that $\Delta g_\epsilon(x)$ with support in the large- x region, the condition $\Delta g_\epsilon(x) \ll \Delta q(x, t)$ is required uniformly in x and t for solutions to be consistent with the positivity condition and with the expectation that $\Delta q(x, t)/q(x, t) \rightarrow 1$ as $x \rightarrow 1$. When this condition is valid, the impact of $\Delta g_\epsilon(x)$ on $A_0^\epsilon(x)$ can be ignored compared with the errors in $\Delta q(x, t)$. Restrictions on parameterizations of $\Delta g_\epsilon(x)$ in the small- x region were found to be much less stringent and as long as the normalization requirement (23) was valid, variations in the shape in the region did not impede the ability to find stable solutions. These studies demonstrate that our approach of parametrizing the shape of $A(x, t)$ can provide an independent, complementary approach to the global fits [15]-[17] directed at the problem of examining the impact of data on $\Delta G(x, t)$ for the determination of $\langle \Delta G(t) \rangle$. In particular, we can formulate consistent parameterizations in which the asymmetry, $A(x, t)$, changes sign.

The phenomenological application of (27) to the determination of $L_z(t_0 = 0)$ implies an understanding of the errors involved in determining the components on the right hand side of (27). In addition to the uncertainty associated with measurements of $\langle \Delta \Sigma \rangle$, which is known explicitly, there are errors associated with

1. the determination of $\langle \Delta G(t) \rangle$ from experiments with limited acceptance,
2. the numerical determination of $A_0^\epsilon(x)$ from solutions to (21) and
3. the continuation to $t = 0$ using $\langle A_0^\epsilon[G(t) - G(0)] \rangle$ within this framework.

We will address the issues in the first two contributions in more detail in section 3. The errors implied by the third point can, in principle, be minimized by solving (14) at NLO in QCD perturbation theory instead of the LO solutions described by (21). This discussion follows here.

2.2 Next-to-leading Order Asymmetry

While we have formulated the arguments above in terms of the solutions to equation (14) using the LO DGLAP equations, it is appropriate at this point to insert a few comments on the application of solutions to the next-to-leading order set of equations

$$\begin{aligned}\Delta G^{NLO}(x, t) &= A_0^{\epsilon, NLO}(x, t_1) \cdot G^{NLO}(x, t) + \Delta g_\epsilon(x) \\ A_0^{\epsilon, NLO}(x, t_1) &\equiv \left[\left(\frac{\partial \Delta G^{NLO}(x, t)}{\partial t} \right) \Big|_{t=t_1} / \left(\frac{\partial G^{NLO}(x, t)}{\partial t} \right) \Big|_{t=t_1} \right]\end{aligned}\quad (28)$$

to the analysis of data sensitive to the polarized gluon asymmetry. Here t_1 is a reference t at NLO. Such phenomenological analyses have traditionally been done in the framework of LO perturbation theory. The non-linear equation analogous to (15) that must be solved numerically then can be written in the form

$$A_0^{\epsilon, NLO}(x, t_1) = \frac{\left[\Delta P_{Gq}^{NLO} \otimes \Delta q^{NLO}(x, t) + \Delta P_{GG}^{NLO} \otimes [A_0^{\epsilon, NLO}(x, t_1) \cdot G^{NLO}(x, t) + \Delta g_\epsilon(x)] \right]}{[P_{Gq}^{NLO} \otimes q^{NLO}(x, t) + P_{GG}^{NLO} \otimes G^{NLO}(x, t)]} \quad (29)$$

where it is specified that the convolutions on the right side are performed with the appropriate distribution functions: $q^{NLO}(x, t)$, $G^{NLO}(x, t)$, $\Delta q^{NLO}(x, t)$, $\Delta G^{NLO}(x, t)$ and the NLO splitting functions all evaluated at $t = t_1$. This specification acknowledges that the splitting functions evaluated at NLO, namely

$$\begin{aligned}\Delta P_{ij}^{NLO}(z, t) &\equiv \Delta P_{ij}^{(0)}(z) + \alpha_s(t) P_{ij}^{(1)}(z) \\ P_{ij}^{NLO}(z, t) &\equiv P_{ij}^{(0)}(z) + \alpha_s(t) P_{ij}^{(1)}(z).\end{aligned}\quad (30)$$

involve a t dependence associated with both the $\bar{M}\bar{S}$ renormalization prescription for $\alpha_s(t)$

$$\alpha_s(t) = e^{-(t-t_1)} \left[1 + b_1(t - t_1) + \dots \right] \quad (31)$$

and with the factorization prescription used in the calculations. It is important to observe that

$$\Delta G^{NLO}(x, t) = \Delta G^{NLO}(x, t_1) + A_0^{\epsilon, NLO}(x, t_1) \cdot [G^{NLO}(x, t) - G^{NLO}(x, t_1)] + \mathcal{O}(\square - \square_\infty)^\epsilon, \quad (32)$$

takes a form analogous to the LO result, except that the corrections $\mathcal{O}(t - t_1)^2$ to (32) are necessarily smaller than those found in (25). In (32), $G^{NLO}(x, t)$ evolves in t with the full

NLO expression while evolution of t in (31) is only approximately correct at NLO. This is, however, an improvement on the LO result. Preliminary numerical calculations indicate that the same methods discussed in section 2.1 above can be used to determine fits of the form

$$A_0^{\epsilon,NLO}(x, t_1) \equiv A(t_1)x^{\alpha(t_1)} - (B(t_1) - 1)x^{\beta(t_1)} + (B(t_1) - A(t_1))x^{\beta(t_1)+1}, \quad (33)$$

to parametrize the shape of $A_0^{\epsilon,NLO}(x, t_1)$.

We have not fully explored the range of boundary conditions defined by different parameterizations of $\Delta g^\epsilon(x)$ for the NLO equations. For parameterizations consistent with (23), we have found that the differences between extrapolations for $\Delta G(x, 0)$ generated at LO and NLO occur primarily for $x \leq 0.10$. It is expected, based on the above discussion, that errors associated with the extrapolation in t of (25) can be improved in NLO. This will be tested in the future. At present, however, we will address issues involving experimental data only at LO.

3 Experimental Extraction of the Gluon Asymmetry and the Orbital Angular Momentum

Section II describes an approach to the determination of $\Delta G(x, t)$ using the decomposition of Eq. (11) combined with experimental information on fits to $q(x, t)$, $G(x, t)$ and $\Delta q(x, t)$ to solve a nonlinear partial differential equation for $A_0^\epsilon(x)$. Since it uses the measured parton distributions in a unique way, this approach is complementary to determination of $\Delta G(x, t)$ based upon a “global analysis” as exemplified in the fits of Hirai and Kumano [15] and as described in other analyses. [16, 17]

In our approach, the function $\Delta g_\epsilon(x)$ describes a boundary condition on the partial differential equation for $A_0^\epsilon(x)$ that represents nonperturbative dynamical constraints on the DGLAP evolution of gluon helicity in a proton. The limits on $\Delta g_\epsilon(x)$ for which stable solutions of Eq. (15) can be found depend sensitively upon the parameterization of the input parton distributions at the specific value of t at which the separation $\Delta G(x, t) = A_0^\epsilon \cdot G(x, t) + \Delta g_\epsilon(x)$ is defined. We have explored those limits using the specific leading order (LO) fits to the input distributions, Eqs. (16)-(20) at $t = 0$ ($Q^2 = 1 \text{ GeV}^2$). This tests the assumption that DGLAP evolution can be combined meaningfully with the $J_z = \frac{1}{2}$

sum rule, Eq. (2), at this scale. The evolution of ΔG depends upon its initial shape, so its determination must be accompanied by assumptions of large- x behavior and interpolations with the small- x shape. Our approach to the shape provides strong theoretical constraints and differs from global fits [15] and models such as the simpler valon model [27], which make different assumptions about the large- x behavior of ΔG .

For those parameterizations of $\Delta g_\epsilon(x)$ for which a stable solution to Eq. (15) exists at $t = 0$, we can insert the decomposition of Eq. (11) into Eq. (13) to write

$$L_z(0) = 0.34 \pm 0.02 - \langle A_0^\epsilon(x) \cdot G(x, 0) \rangle - \langle \Delta g_\epsilon(x) \rangle \quad (34)$$

and evolve the equivalent possible forms of $\Delta G(x, 0)$ to compare with experimental extractions of $\Delta G(x, t)$ found through processes such as prompt photon and photon + jet measurements. The terms in Eq. (34) use the experimental averages for $\langle \Delta \Sigma \rangle$ from COMPASS and HERMES, and the CTEQ or MRST parameterizations for $G(x, t_0)$ from section II. The error quoted here is due to the uncertainties in the data, as previously mentioned and the small theoretical uncertainties associated with the unpolarized distributions. For those asymmetry parameterizations that best agree with data, we can extract the most likely range for the orbital angular momentum of the constituents.

From these results, a strictly theoretical approach to finding feasible values to L_z yields a range allowed by the “practical” constraints of

$$\begin{aligned} -0.12 &\leq \langle \Delta G \rangle \leq 0.62 \quad \text{and} \\ -0.28 &\leq L_z(0) \leq 0.46, \end{aligned} \quad (35)$$

where the theoretical and experimental uncertainties have been included in the quoted inequality values. The range is not sensitive to the unpolarized input distributions and the corresponding theoretical uncertainties have been included in this range. The ranges of $\langle \Delta G \rangle$ and $\langle L_z \rangle$ appear to be numerically limited by the constraints on $\langle \Delta g_\epsilon \rangle$ in equation (23). From a theoretical point of view, this results in relatively small values of ΔG and L_z , but the range is still considerable. We must use the data on the asymmetry to further narrow the possible values of the gluon polarization and the orbital angular momentum. Table 3 includes a summary of present data on the asymmetry [1-5].

It is virtually impossible to find parameterizations that completely agree with all data. Two separate analyses were performed: a χ^2 calculation of all parameterizations with all

Table 2: Measurements of the gluon asymmetry

Experiment	Process	Value	stat	sys	x_{avg}	Comment
COMPASS	open charm	-0.49	± 0.27	± 0.11	0.11	Large errors
COMPASS	High p_T hadrons	0.016	± 0.058	± 0.055	0.09	$Q^2 \geq 1 \text{ GeV}^2$
COMPASS	High p_T hadrons	-0.06	± 0.31	± 0.06	0.13	$Q^2 \leq 1 \text{ GeV}^2$
SMC	High p_T hadrons	-0.20	± 0.28	± 0.10	0.07	$Q^2 \geq 1 \text{ GeV}^2$
HERMES	Factorization method	0.078	± 0.034	± 0.011	0.204	Consistent with RHIC
HERMES	Approximation method	0.071	± 0.034	± 0.010	0.222	Consistent with RHIC
HERMES	High p_T hadrons	0.41	± 0.18	± 0.03	0.17	$Q^2 \leq 1 \text{ GeV}^2$

existing data and a determination of which of the asymmetry parameterizations best agreed to within one to two σ of the data set in Table 2. Six of the parameterizations in Table one, corresponding to lines 1, 2, 4, 6, 7 and 9 all minimized χ^2 and were within 2σ for at least five of the seven data points. All of the parameterizations that best agree with data have the property that $\Delta g_e \leq 0$. A plots showing four of the parameterizations of $A(x, t_0)$ at LO are shown in figure 1.

Using only these parameterizations, the range of ΔG and L_z that result are

$$-0.12 \leq \langle \Delta G \rangle \leq 0.31 \quad \text{and} \quad (36)$$

$$0.03 \leq L_z(0) \leq 0.46, \quad (37)$$

where, again, the uncertainties are included in the extreme values. These results are consistent with data and the MIT Bag model, discussed by Chen and Ji. [12] Using present data, the range of ΔG and L_z have been narrowed, but clearly, accurate data over a wider kinematic range can more significantly constrain both the gluon polarization and the orbital angular momentum of the constituents. The results for the scenarios we have shown are not significantly different from each other. However, we do not rule out the necessity of altering this approach to consider more flexible parameterizations if data change significantly. We consider it likely that additional accurate data for the gluon asymmetry and ΔG over a wider kinematic range will allow us to further restrict our range of consistency. Two immediate experimental possibilities are

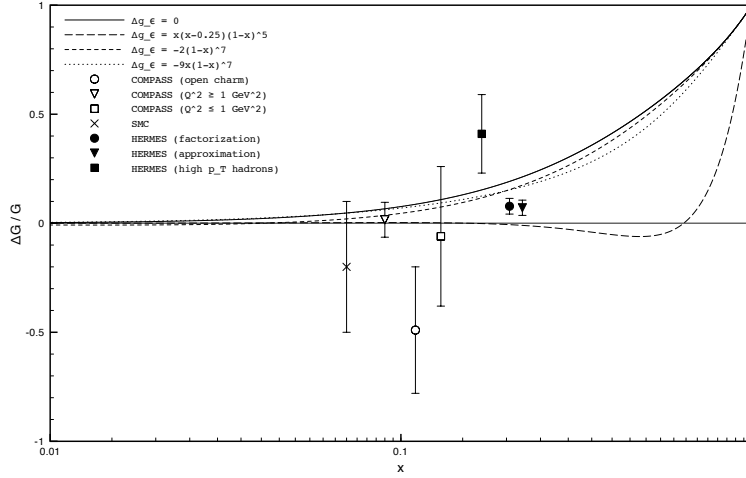


Figure 1: The existing data for the polarized gluon asymmetry with the parameterizations that best agree with data.

- (1) the measurement of $\Delta G/G$ in a wider kinematic range of x_{Bj} for a fixed Q_0^2 value and
- (2) extraction of ΔG by prompt photon production or jet production in polarized pp collisions (RHIC).

Our results indicate that the integrated $\langle \Delta G \rangle$ is likely positive and small at $Q_0^2 \approx 1$ GeV^2 . This is consistent with data [1, 5], chiral quark models [28] and the MIT bag model [12]. Although most of our parameterizations of the asymmetry are positive definite, the one in the second line of Table 2 changes sign and is consistent with data. This possibility has been discussed by others and is not ruled out by present data [12, 15, 29]. Many of our parameterizations give a gluon polarization consistent with zero, in agreement with much of the data from RHIC. [3, 4] Clearly there is still work to be done. However, we have provided a mechanism for calculating the gluon asymmetry that allows extraction of information on both ΔG and L_z .

In Table 3, we outline some of the (mostly quark) models that make predictions about the orbital angular momentum of the constituents (nearly all L_z^q contributions). This includes various quark models combined with corresponding gluon scenarios. Most fall within the same range as our calculations, except those predicting a large orbital angular momentum, either positive or negative. However, ours is a purely phenomenological approach that

Table 3: Comparison of Orbital Angular Momentum Models

Model	L_z at $Q_0^2 = 1 \text{ GeV}^2$	Reference	Notes
CQSM	$0.25 - 0.32$	[30]	$\mu_0^2 = 600 \text{ MeV}^2$, no gluons
CQSM	0.25	[31]	$J_G \approx 0$, $L_q \leq \frac{1}{3}$
R χ QM model	0.25	[31]	$\Delta G \leq 0.10$
χ QM	0.26	[32]	no gluons, all L_z^q
Skyrme	0.50	[32, 33]	no gluons
Casu-Seghal	0.42	[34]	
IK Quark model	-0.25	[35]	$\Delta G = 0.59$, $L_z \approx L_q$
MIT Bag	0.18	[12, 32]	$\Delta G : 0.2 - 0.3$
RGM+OGE+ π cloud	$0.35 - 0.61$	[36]	L_q contribution only
Quark model	-0.43	[37]	Maximal glue - GRSV
Quark model	0.025	[37]	Normal GRSV glue
Lattice calculation	0.38	[38]	Unquenched: no glue

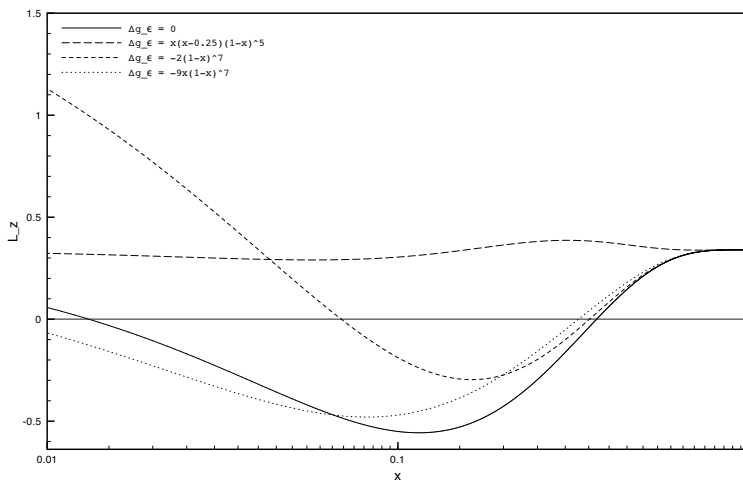


Figure 2: Orbital angular momenta as a function of x for parametrizations of the polarized gluon asymmetry that best agree with data.

includes gluon contributions extracted from the asymmetry and does not rely entirely on present fits to data. We use the data only to constrain those models which are most viable. Clearly, accurate data in a wider kinematic range of x and Q^2 are necessary to distinguish those models that are most viable and determine the total angular momentum of the constituents.

For illustrative purposes, we have shown a plot of the x -dependent function, $L_z(x, t = 0)$ in figure 2 for those parametrizations of Δg_ϵ included in figure 1. Note that they have different behavior at small- x , further motivating the need for accurate asymmetry data, especially at these values of x .

To summarize the relation between allowable values of ΔG and the orbital angular momentum of constituents, figure 3 shows the range of ΔG values determined by our analysis and the corresponding range of L_z values, bounded by the vertical lines.

4 Conclusion

The property of color confinement implies that, at distance scales on the order of hadron sizes, the effective dynamic degrees of freedom for hadronic interactions are not given directly by perturbative interactions of quarks and gluons, but by some variety of collective excitations of the objects. Computer simulations of lattice regularized QCD have proven to be an

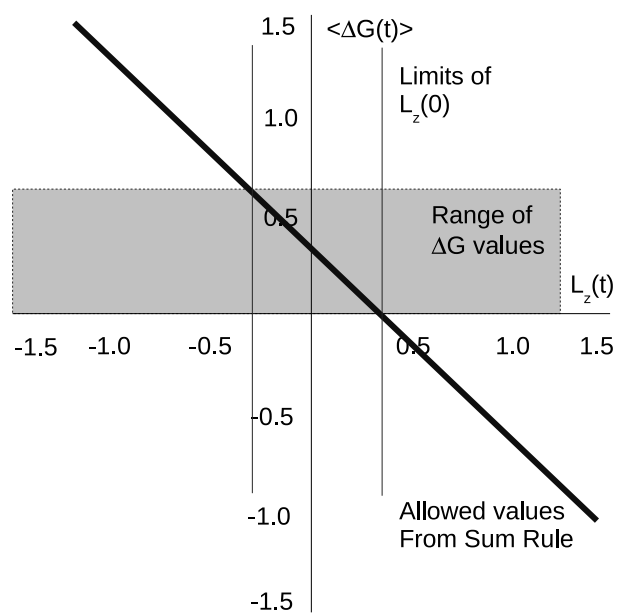


Figure 3: Possible range of ΔG values as a function of the orbital angular momentum L_z .

effective tool for understanding many aspects of the crucial distance scale [41]. In addition, the implications of the broken chiral symmetry of QCD associated with the light quark masses has been incorporated into a class of effective field theories for the pseudo-Goldstone bosons [42] of the broken symmetry. This process has led to descriptions of nuclear structure such as the Georgi-Manohar chiral quark model [40] or versions of the chiral quark soliton model, originated by Wess and Zumino [43] in the treatment of the Skyrme solution. [33]

Our approach to the study of the gluon asymmetry presented in sections 2 and 3 has applied the $J_z = \frac{1}{2}$ rule and focussed on the ability to use information on $\Delta G(x, t)$ to estimate the orbital angular momentum $L_z(t)$ at low energy scales. This is due to the features of proton structure that can be described in terms of the constituent quark model involving non-relativistic “constituent” quarks in an s -wave $L = 0$ state. In this context, nonzero orbital angular momentum of colored constituents as inferred from equation (13) is associated with the internal structure of the constituent quarks. The importance of such virtual corrections can also be studied in the flavor asymmetry of the $q\bar{q}$ sea, [44] but the knowledge of $L_z(t)$ at values of $Q^2 = 1 \text{ GeV}^2$ provides more complete information. For example, the orbital angular momentum of constituents in the Georgi-Manohar model has been studied by Song [32] and Sivers [45]. Song’s results of $L_z = 0.30$ are based upon a true effective field theoretical approach and does not consider the impact of gluons. The approach of reference [45] estimates the impact of gluonic orbital angular momentum in Song’s approach by requiring consistency between transverse and longitudinal spin. The results there are $L_z = 0.39 \pm 0.02$.

We have described a decomposition of the scale-dependence of the gluon spin asymmetry, $\Delta G(x, t)$. This approach allows a measurement sensitive to $\Delta G(x, t)$ to be extrapolated in a manner consistent with DGLAP evolution, counting rules and the measured distributions $\Delta q(x, t)$, $q(x, t)$ and $G(x, t)$ to help complete a more comprehensive dynamical picture of nucleon spin structure. The numerical work with the leading-order approximation to this equation indicates that the range of stability is acceptable. Furthermore, existing experimental measurements, within reported errors suggest that $\Delta G(x, t)$ lies within this range. To illustrate the value of this decomposition, we have considered the orbital angular momentum inferred from the $J_z = \frac{1}{2}$ sum rule.

References

- [1] A. Airpetian, *et al.*, Phys. Rev. Lett. **84**, 2584 (2000) (HERMES Collaboration)
- [2] B. Adeva, *et al.*, (Spin Muon Collaboration), Phys. Rev. **D70**, 012002 (2004)
- [3] B I Abelev, *et al.*, Phys. Rev. Lett. **97**, 252001 (2006) and R Fatemi, arXiv:0710.3207 [hep-ex] (STAR Collaboration)
- [4] A. Adare, *et al.*, Phys. Rev. **D76**, 051106 (2007) and S. S. Adler, *et al.*, Phys. Rev. **D73**, 091102 (2006) (PHENIX Collaboration)
- [5] M. Alekseev, *et al.*, Phys. Lett. **B676**, 31 (2009) (COMPASS Collaboration)
- [6] J. Babcock, E. Monsay and D. Sivers, Phys. Rev. **D19**, 1483 (1979)
- [7] R. L. Jaffe and A. Manohar, Nucl. Phys. **B337**, 509 (1990)
- [8] X. Ji, split of q and G Lz asymptotically
- [9] P. Ratcliffe, Phys. Lett. **B192**, 180 (1987)
- [10] G. Altarelli and G. Parisi, Nucl. Phys. **B126**, 298 (1977); Dokshitzer; V.N. Gribov and L.N. Lipatov, Yad. Fiz.,**15**, 781 (1972) and Sov. J. Nucl. Phys.,**15**, 438 (1972).
- [11] B. L. G. Bakker, E. Leader and T. L. Trueman, Phys. Rev. **D70**, 114001 (2004)
- [12] P. Chen and X. Ji, Phys. Lett. **B660**, 193 (2008); X. Ji, arXiv:0810.4913 [hep-ph] and references therein
- [13] A. Airpetian, *et al.*, Phys. Rev. **D75**, 012007 (2007) (HERMES Collaboration)
- [14] F. Bradamante, Phys. Lett. **B612**, 154 (2005) and Prog. Part. Nucl. Phys. **61**, 229 (2008) and Phys. Lett. **647**, 8 (2007); M. Alekseev, *et al.*, Phys. Lett. **B647**, 8 (2007) and Phys. Lett. **B660**, 458 (2008) and arXiv: 0707.4077 [hep-ex] (COMPASS Collaboration)
- [15] M. Hirai, S. Kumano and N. Saito, (AAC) Phys Rev D69, 054021 (2004), M. Hirai and S. Kumano, Nucl. Phys. B813, 106 (2009) and M Hirai and S Kumano, arXiv:0808.0413 [hep-ph] KEK-TH-1208

- [16] M. Burkardt, C. A. Miller and W-D Nowak, arXiv:0812.2208v3 [hep-ph], DESY 08-162, JLAB-THY-08-913
- [17] J. Blumlein and H. Bottcher, Nucl. Phys. **B636**, 225 (2002)
- [18] M. Einhorn, Proc. of the Workshop on Polarized Beams at SSC, Ann Arbor 1985, p. 149 (1985). See also M. Einhorn and J. Soffer, Nucl. Phys. **B274**, 714 (1986)
- [19] F. E. Close and D. Sivers, Phys. Rev. Lett. **39**, 1116 (1977).
- [20] G.P. Ramsey, AIP Proceedings 570, 437 (2001), proceedings of SPIN 2000, Osaka, Japan, Eds. K. Hatanaka, T. Nakano, K. Imai and H. Ejiri., hep-ph/0101044 and Int. J. Mod. Phys., 18, 1211 (2003), hep-ph/0201041.
- [21] G. P. Ramsey, Proceedings of DSPIN-05, Dubna, Russia, Ed., A. V. Efremov, c2006, World Scientific, p. 120 and arXiv: hep-ph/0601141
- [22] G. P. Ramsey, Y. Binder and D. Sivers, ANL-HEP-CP-08-1, Proceedings of DSPIN-07, Dubna, Russia, Eds., A. V. Efremov and S. V. Goloskokov, c2008, World Scientific, p. 138 and arXiv: 0801:1128 [hep-ph]
- [23] G. P. Ramsey, p. 353, AIP Conference Proceedings 1149, SPIN-2008, University of Virginia, Charlottesville.
- [24] CTEQ Collaboration, H. L. Lai *et al.*, Eur. Phys. J., **C12**, 375 (2000) and hep-ph/9903282; D. Stump, *et. al.*, Phys. Rev. **D65**, 014012 (2002).
- [25] MRST Collaboration, A. D. Martin *et al.*, Eur. Phys. J., **C4**, 463 (2008).
- [26] L. E. Gordon, M. Goshtasbpour and G. P. Ramsey Phys. Rev. **D58**, 094017 (1998) and hep-ph/9803351.
- [27] A. Shahveh, F. Taghavi-Shahri, F. Arash, Phys. Lett. **B691**, 32 (2010).
- [28] M. Wakamatsu, Phys. Lett. **B646**, 24 (2007)
- [29] E. Leader, A. Siderov and D. Stamenov, Phys. Rev. **D75**, 074027 (2007)
- [30] M. Wakamatsu, AIP Conf. Proc. **915**, 630 (2007), SPIN 2006, Kyoto, Japan.

- [31] P. Zavada, hep-ph/0511142, Workshop on Nucleon Form Factors, Frascati, 2005
- [32] X. Song, hep-ph/9801332, INPP-UVA-97-07 and Phys. Rev. **D57**, 4114 (1998), hep-ph/9712351.
- [33] T.H.R. Skyrme, Nucl. Phys. **31**, 556 (1962).
- [34] M. Casu and L.M.Seghal, Phys. Rev. **D55**, 2644 (1997)
- [35] V. Barone, T. Calarco and A. Drago, Phys. Lett. **B431**, 405 (1998)
- [36] A. W. Thomas, Int. J. Mod. Phys., **E18**, 1116 (2009), arXiv 0904:1735 (hep-ph)
- [37] O. Martin, P. Hagler and A. Schafer, Phys. Lett. **B448**, 99 (1999) and hep-ph/9810474.
- [38] E. Santopinto and R. Bijker, Proceedings of the 11th Workshop on Physics of Excited Nucleons, NSTAR 2007, 35-39, Springer (2008), arXiv 0809.2296 [nucl-th].
- [39] R. D. Ball, S. Forte and G. Ridolfi, Nucl. Phys. **B444**, 287 (1996) and Phys. Lett. **B378**, 255 (1996).
- [40] A. Manohar and H. Georgi, Nucl. Phys. **B234**, 189 (1984)
- [41] See for example, H. J. Rothe, Lattice Gauge Theories: An Introduction, World Scientific Lecture Notes in Physics **74**, (2005).
- [42] See for example, H. Leutwyler, Handbook of QCD: Vol I, World Scientific (2001)
- [43] J. Wess and B. Zumino, Phys. Lett. **B37**, 95 (1971).
- [44] E.J. Eichten, I. Hinchcliffe and C. Quigg, Phys. Rev. **D45**, 2269 (1992).
- [45] D. Sivers, ArXiv: 0704.1791 (hep-ph).